

Let's keep brainstorming title ideas. I don't think our results support the idea of 'episodes of rapid expansion'

Trevor Drees<sup>\*a,b</sup>, Brad M. Ochocki<sup>b</sup>, Scott L. Collins<sup>c</sup>, and Tom E.X. Miller<sup>b</sup>

<sup>a</sup>Department of Biology, Penn State University, State College, PA USA

<sup>b</sup>Program in Ecology and Evolutionary Biology, Department of BioSciences, Rice University, Houston, TX USA

<sup>c</sup>Department of Biology, University of New Mexico, Albuquerque, NM USA

April 12, 2021

---

\*thd5066@psu.edu

# 1 Abstract

2 **Encroachment**<sup>1</sup> of shrubs into adjacent grasslands has become an increasingly reported  
3 phenomenon across the world, and such encroachment is either pulled forward by high  
4 population growth at the low-density encroachment front or pushed forward by higher-  
5 density areas behind the front. However, at sites such as Sevilleta National Wildlife  
6 Refuge in central New Mexico, little is known about whether encroachment is pushed or  
7 pulled, and the dynamics of encroachment are not well-understood. Here, long-term en-  
8 croachment of creosotebush (*Larrea tridentata*), a native perennial shrub, stands in stark  
9 contrast with the stagnation in encroachment observed in recent decades. In order to  
10 better understand creosotebush encroachment at this site, we quantify it using a spatially  
11 structured population model where a wave of individuals travels at a speed governed by  
12 both dispersal and density-dependence. Results indicate that population growth rates  
13 generally increase with decreasing density, suggesting that encroachment is pulled by  
14 individuals at the low-density wave front, and the spatial population model predicts an  
15 encroachment rate of less than 2 cm per year. While the predicted rate of encroach-  
16 ment is consistent with observations over recent decades, it does not explain long-term  
17 creosotebush encroachment at the study site, suggesting that this process may occur in  
18 pulses when recruitment, seedling survival, or dispersal significantly exceed typical rates.  
19 Overall, our work demonstrates that individuals at low densities are likely the biggest  
20 contributors to creosotebush encroachment at this site, and that this encroachment is  
21 likely a process that occurs in large but infrequent bursts rather than at a steady pace.

## 22 Keywords

23 density-dependence, ecotones, woody encroachment, shrubs, integral projection model,  
24 grassland

---

<sup>1</sup>*I am not editing the abstract for now.*

## 25 Introduction

26 The recent and ongoing encroachment of shrubs and other woody plants into adjacent  
27 grasslands has caused significant vegetation changes across arid and semi-arid landscapes  
28 worldwide (Van Auken, 2000, 2009; Goslee et al., 2003; Gibbens et al., 2005; Parizek et al.,  
29 2002; Cabral et al., 2003; Trollope et al., 1989; Roques et al., 2001). The process of en-  
30 croachment generally involves increases in the number or density of woody plants in both  
31 time and space (Van Auken, 2000), which can drive shifts in plant community structure  
32 and alter ecosystem processes (Schlesinger et al., 1990; Ravi et al., 2009; Schlesinger  
33 and Pilmanis, 1998; Knapp et al., 2008). Other effects of encroachment include changes  
34 in ecosystem services (Reed et al., 2015; Kelleway et al., 2017), declines in biodiversity  
35 (Ratajczak et al., 2012; Sirami and Monadjem, 2012; Brandt et al., 2013), and economic  
36 losses in areas where the proliferation of shrubs adversely affects grazing land and pastoral  
37 production (Mugasi et al., 2000; Oba et al., 2000).

38 Woody plant encroachment can be studied through the lens of spatial population  
39 biology as a wave of individuals that may expand across space and over time (Kot et al.,  
40 1996; Neubert and Caswell, 2000; Wang et al., 2002; Pan and Lin, 2012). Theory pre-  
41 dicts that the speed of wave expansion depends on two processes: local demography and  
42 dispersal of propagules. First, local demographic processes include recruitment, survival,  
43 growth, and reproduction, which collectively determine the rate at which newly colonized  
44 locations increase in density and produce new propagules. Second, colonization events  
45 are driven by the spatial dispersal of propagules, which is commonly summarized as a  
46 probability distribution of dispersal distance, or “dispersal kernel”. The speed at which  
47 expansion waves move is highly dependent upon the shape of the dispersal kernel, espe-  
48 cially long-distance dispersal events in the tail of the distribution (Skarpaas and Shea,  
49 2007). Both demography and dispersal may depend on plant size, since larger plants  
50 often have improved demographic performance and release seeds from greater heights,

51 leading to longer dispersal distances (Nathan et al., 2011). Accounting for population  
52 structure, including size structure, may therefore be important for understanding and  
53 predicting wave expansion dynamics (Neubert and Caswell, 2000).

54 Theory predicts that the nature of conspecific density dependence is another critical  
55 feature of expansion dynamics but this is rarely studied in the context of woody plant  
56 encroachment. Expansion waves typically correspond to gradients of conspecific density  
57 – high in the back and low at the front – and demographic rates may be sensitive to  
58 density due to intraspecific interactions like competition or facilitation. If the demo-  
59 graphic effects of density are strictly negative due to competitive effects that increase  
60 with density then demographic performance is maximized as density goes to zero, at the  
61 leading edge of the wave. Under these conditions, the wave is “pulled” forward by indi-  
62 viduals at the low-density vanguard (Kot et al., 1996), and targeting these individuals  
63 and locations would be the most effective way to slow down or prevent encroachment  
64 (cite?). However, woody encroachment systems often involve positive feedbacks whereby  
65 shrub establishment modifies the environment in ways that facilitate further shrub re-  
66 cruitment. For example, woody plants can modify their micro-climates in ways that  
67 elevate nighttime minimum temperatures, promoting conspecific recruitment and sur-  
68 vival for freeze-sensitive species (D’Odorico et al., 2010; Huang et al., 2020). Such Allee  
69 effects (in the language of population biology) cause demographic rates to be maximized  
70 at higher densities behind the leading edge, which “push” the expansion forward, leading  
71 to qualitatively different dynamics (Kot et al., 1996; Taylor and Hastings, 2005; Sullivan  
72 et al., 2017; Lewis and Kareiva, 1993; Veit and Lewis, 1996; Keitt et al., 2001). Pushed  
73 expansion waves generally have different shapes (steeper density gradients) and slower  
74 speeds than pulled waves (Gandhi et al., 2016), and may require different strategies for  
75 managing or decelerating expansion (check Taylor and Hastings ref). The potential for  
76 positive feedbacks is well documented in woody encroachment systems but it remains  
77 unclear whether and how strongly these feedbacks decelerate shrub expansion and influ-

78   ence strategies for management of woody encroachment. Despite decades of work on this  
79   topic, we still do not know whether expansion waves of woody encroachment are pushed  
80   or pulled.

81       In this study, we linked woody plant encroachment to ecological theory for invasion  
82   waves, with the goals of understanding how seed dispersal and density-dependent demog-  
83   raphy drive encroachment, and determining whether the encroachment wave is pushed or  
84   pulled. Throughout the aridlands of the southwestern United States, shrub encroachment  
85   into grasslands is well documented (cite) but little is known about the dispersal and de-  
86   mographic processes that govern it. Our work focused on encroachment of creosotebush  
87   (*Larrea tridentata*) in the northern Chihuahuan Desert. Expansion of this species into  
88   grasslands over the past 150 years has been well documented, leading to decreased cover  
89   of *Bouteloua eriopoda*, the dominant foundation species of Chihuahuan desert grassland  
90   (Gardner, 1951; Buffington and Herbel, 1965; Gibbens et al., 2005). As in many woody  
91   encroachment systems, creosotebush expansion generates ecotones marking a transition  
92   from dense shrubland to open grassland, with a transition zone in between where shrubs  
93   can often be found interspersed among grasses (Fig. 1).

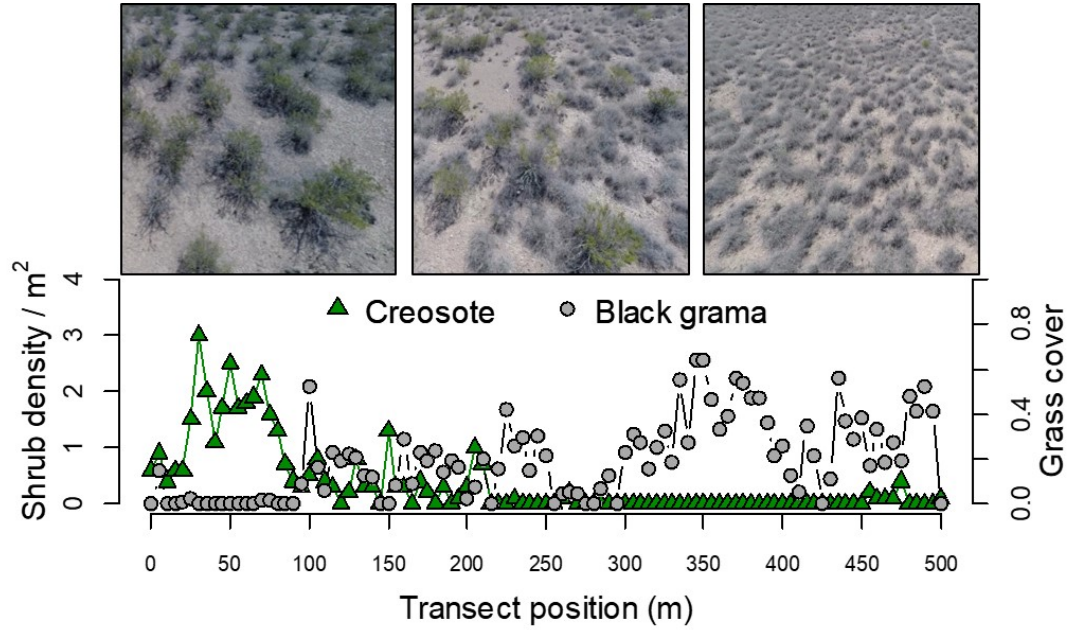


Figure 1: Caption.

Historically, creosotebush encroachment into grasslands is believed to have been driven by a combination of factors including overgrazing, drought, variability in rainfall, and suppression of fire regimes Moreno-de las Heras et al. (2016). These shrubs are also thought to further facilitate their own encroachment through positive feedbacks (Grover and Musick, 1990; D’Odorico et al., 2012) by modifying their environment in ways that favor continued growth and recruitment, such as the local micro-climate (D’Odorico et al., 2010) and rates of soil erosion (Turnbull et al., 2010). Such positive feedback also involve suppression of herbaceous competitors, reducing competition as well as the amount of flammable biomass used to fuel the fires that keep creosotebush growth in check (Van Auken, 2000). We hypothesized that, given potential for positive feedback mechanisms, the rarity of conspecifics at the low-density encroachment front may depress demographic performance and generate pushed-wave dynamics.

We used a combination of observational and experimental data from shrub ecotones

107 in central New Mexico to parameterize a spatial integral projection model (SIPM) that  
108 predicts that speed of encroachment ( $m/yr$ ) resulting from lower-level demographic and  
109 dispersal processes. Our data came from demographic surveys and experimental trans-  
110 plants along replicate ecotone transects spanning a gradient of shrub density and seed  
111 drop experiments to infer the properties of the dispersal kernel. We focused on wind  
112 dispersal of seeds as a starting point, since little is known about the natural history  
113 of dispersal in this system and the seeds lack rewards to attract animal dispersers. We  
114 also used re-surveys of permanent transects as an independent measure of encroachment  
115 that provided a benchmark against which to evaluate model predictions. The SIPM ac-  
116 counts for size-structured demography of creosotebush, allows us to test whether shrub  
117 expansion is pulled by the low-density front or pushed from the high-density core, and  
118 identifies the local (demographic) and spatial (seed dispersal) life cycle transitions that  
119 most strongly contribute to expansion speed<sup>2</sup>. We address the following specific ques-  
120 tions:

- 121 1. What is the observed rate of creosotebush encroachment in recent past?
- 122 2. How do creosotebush size and conspecific density affect variation in demographic  
123 vital rates (survival, growth, reproduction, and recruitment) along shrub encroach-  
124 ment ecotones?
- 125 3. What is the wind dispersal kernel for this species and how far do seeds typically  
126 travel by wind?
- 127 4. What is the predicted rate of expansion from the SIPM and what lower-level pro-  
128 cesses most strongly govern the expansion speed?
- 129 5. Is encroachment pulled by the individuals at the front of the wave or pushed by  
130 individuals behind it?

---

<sup>2</sup>*we will need to stay consistent with the language of encroachment/expansion/invasion. For now I am swictihg a lot.*

## 131 **Materials and methods**

### 132 **Study species**

133 Creosotebush *Larrea tridentata* is a perennial, drought-resistant shrub that is native to  
134 the arid and semiarid regions of the southwestern United States and northern Mexico.  
135 These shrubs are often found in valleys and on dunes and gentle slopes (Marshall, 1995).  
136 High-density areas of creosotebush consist largely of barren soil between plants due to  
137 the “islands of fertility” these shrubs create around themselves (Schlesinger et al., 1996;  
138 Reynolds et al., 1999), though lower-density areas will often contain grasses in the in-  
139 tershrub spaces (Fig. 1). In our northern Chihuahuan desert study region creosotebush  
140 reproduces sexually, with numerous small yellow flowers giving rise to highly pubescent  
141 spherical fruits several millimetres in diameter; these fruits consist of five carpels, each  
142 of which consists of a single seed. Seeds are dispersed from the parent plant by gravity  
143 and wind, with the possibility for seeds to also be blown across the soil surface or trans-  
144 ported by water runoff (Maddox and Carlquist, 1985). In other regions, this species also  
145 reproduces asexually and can give rise to long-lived clonal stands (Vasek, 1980), but this  
146 does not occur in our study region. The foliage is dark green, resinous, and unpalatable  
147 to most grazing and browsing animals (Mabry et al., 1978).

### 148 **Study site**

149 We conducted our experiments and censuses at the Sevilleta National Wildlife Refuge  
150 (SNWR), a Long-Term Ecological Research (LTER) site in central New Mexico. The  
151 refuge exists at the intersection of several eco-regions, including the Chihuahuan Desert  
152 and steppes of the Colorado Plateau. Annual precipitation is low at approximately  
153 250 mm, with the majority falling during the summer monsoon season from June to  
154 September.

155 Significant creosotebush encroachment at SNWR is believed to have last occurred



156 in the 1950's, with high shrub recruitment before and after a multi-year drought that  
157 caused a large loss in grass cover, setting the stage for creosotebush expansion (Moreno-  
158 de Las Heras et al., 2015; Moreno-de las Heras et al., 2016). The recruitment events  
159 that facilitate creosotebush expansion are thought to be highly episodic (Peters and Yao,  
160 2012). Given that creosotebush seedlings have been shown to establish around the time  
161 that late-summer heavy rainfall occurs (Boyd and Brum, 1983; Bowers et al., 2004),  
162 higher precipitation rates may be responsible for increased recruitment.

### 163 **Encroachment re-surveys**

164 We recorded shrub percent cover along two permanent 1000-m transects that spanned  
165 the shrub-grass ecotone, from high to low to near-zero shrub density. These surveys were  
166 conducted in summer 2001 and again in summer 2013 to document change in creosotebush  
167 abundance and spatial extent. At every 10 meters, shrub cover was recorded in nine cover  
168 classes (<1%, 1–4%, 5–10%, 10–25%, 25–33%, 33–50%, 50–75%, 75–95%, >95%). For  
169 visualization, we show midpoint values of these cover classes at each meter location for  
170 both transects and years.

### 171 **Demographic data**

#### 172 **Ecotone transects**

173 Collection of demographic data occurred during early June of every year from 2013-  
174 2017. This work was conducted at four sites in the eastern part of SNWR (one site  
175 was initiated in 2013 and the other three in 2014), with three transects at each site.  
176 All transects were placed along a shrubland-grassland ecotone so that a full range of  
177 shrub densities was captured: each transect spanned core shrub areas, grassland with  
178 few shrubs, and the transition between them. Lengths of these transects varied from  
179 200 to 600 m, determined by the strength of vegetation transition, as “steep” transitions  
180 required less length to capture the full range of shrub densities.

181 We quantified shrub density in 5-meter “windows” along each transect, including  
182 plants within one meter of the transect on either side. Densities were quantified once for  
183 each transect (in 2013 or 2014) and were assumed to remain effectively constant for the  
184 duration of the study, a reasonable assumption for a species with very low recruitment  
185 and very high survival of established plants. Given the population’s size structure, we  
186 weighted the density of each window by the sizes of the plants, which we quantified as  
187 volume ( $\text{cm}^3$ ). Volume was calculated as that of an **elliptic**<sup>3</sup> cone:  $V_i = \pi lwh/3$  where  $l$ ,  
188  $w$ , and  $h$  are the maximum length, maximum width, and height, respectively. Maximum  
189 length and width were measured so that they were always perpendicular to each other,  
190 and height was measured from the base of the woody stem at the soil surface to the  
191 highest part of the shrub. The weighted density for a window was then expressed as  
192  $\log(\text{volume})$  summed over all plants in the window.

### 193 **Observational census**

194 At 50-m intervals along each transect we tagged up to 10 plants for annual demographic  
195 census and recorded their local (5-m resolution) window, so that we could connect in-  
196 dividual demographic performance to local weighted density. These tagged shrubs were  
197 revisited every June and censused for survival (alive/dead), size (width, length, and  
198 height, as above), and reproduction (numbers of flowers and fruits). In instances where  
199 shrubs had large numbers of reproductive structures that would be difficult to reliably  
200 count, we made counts on a fraction of the shrub and extrapolated to estimate whole-  
201 plant reproduction. Each year, we also searched for new recruits within one  $m$  on either  
202 side of the transect. New recruits were tagged and added to the demographic census.

---

<sup>3</sup>*I checked the code and actually this is not what we did.*

## 203 Transplant experiment

## 204 Demographic data analysis

205 Collected demography data were then examined to investigate how weighted density  
206 and shrub volume affected four different demographic variables: survival, probability  
207 of flowering (i.e. producing at least one flower or fruit), annual growth, and number of  
208 reproductive structures. Each of these demographic variables was fit to a different mixed-  
209 effects model through maximum likelihood. Both survival and probability of flowering  
210 were each fit to generalised linear mixed-effects models using a binomial response and a  
211 logit link function. Annual growth was defined as  $\ln(V_{t+1}/V_t)$  where  $V_{t+1}$  and  $V_t$  are the  
212 shrub volumes in the current and previous years, respectively, and was then fit to a linear  
213 mixed-effects model. The number of reproductive structures was defined as the natural  
214 logarithm of the sum of fruits and flowers on the entire shrub and was fit to a linear  
215 mixed-effects model as well. To construct these models, all of the equations listed in  
216 Table 1 were first fit to each of the four demographic variables, with each equation using  
217 volume and standardised density as predictors while also treating the unique transect  
218 in which each shrub was located as a random effect. After these equations were fit to  
219 the data, all eight equations for each demographic variable were ranked based on their  
220 value of the Akaike information criterion (AIC) and weighted based on their quality so  
221 that better-fitting models had a higher weight. Then, coefficients of the same type were  
222 averaged between all eight models for each demographic variable using a weighted mean  
223 corresponding to model quality in order to generate an average model. All four average  
224 models have the general form

$$225 \quad R = \beta_1 v + \beta_2 d + \beta_3 d^2 + \beta_4 vd + \beta_5 vd^2 + \epsilon \quad (1)$$

226 where  $R$  is the response variable,  $v$  and  $d$  are the volume and density,  $\epsilon$  is a random  
227 transect effect, and  $\beta$  is the coefficient for each type of term.

228 The effect of density dependence on the probability of recruitment from seeds was  
 229 also modelled. For every year, the sum of seeds produced the prior year was calculated  
 230 for each 5-m subsection, and then probability of recruitment was calculated as the num-  
 231 ber of recruits observed in each 5-m subsection divided by that number of seeds. For  
 232 any subsection in which seeds were not found, a count of seeds was estimated based on  
 233 the number of seeds in a subsection of similar weighted density; this was done to avoid  
 234 creating any undefined values of recruitment probability. Both linear and quadratic mod-  
 235 els using only weighted density as a predictor were fit to the distribution of recruitment  
 236 probabilities, though the linear model was ultimately used because it had a higher AIC  
 237 value.

## 238 **Dispersal modelling**

239 Dispersal kernels were calculated using the WALD, or Wald analytical long-distance  
 240 dispersal, model that uses a mechanistic approach to predict dispersal patterns of plant  
 241 propagules by wind. The WALD model, which is largely based in fluid dynamics, can  
 242 serve as a good approximation of empirically-determined dispersal kernels (Katul et al.,  
 243 2005; Skarpaas and Shea, 2007) and may be used when empirical dispersal data is not  
 244 readily available. Under the assumptions that wind turbulence is low, wind flow is  
 245 vertically homogenous, and terminal velocity is achieved immediately upon seed release,  
 246 the WALD model simplifies a Lagrangian stochastic model to create a dispersal kernel  
 247 that estimates the likelihood a propagule will travel a given distance (Katul et al., 2005).  
 248 This dispersal kernel takes the form of the inverse Gaussian distribution

$$249 \quad p(r) = \left( \frac{\lambda'}{2\pi r^3} \right)^{\frac{1}{2}} \exp \left[ -\frac{\lambda'(r - \mu')^2}{2\mu'^2 r} \right] \quad (2)$$

250 that is a slight adaptation from equation 5b in Katul et al. (2005), using  $r$  to denote  
 251 dispersal distance. Here,  $\lambda'$  is the location parameter and  $\mu'$  is the scale parameter,

252 which depend on environmental and plant-specific properties of the study system. The  
 253 location and scale parameters are defined as  $\lambda' = (H/\sigma)^2$  and  $\mu' = HU/F$ ; these are  
 254 functions of the height  $H$  of seed release, wind speed  $U$  at seed release height, seed  
 255 terminal velocity  $F$ , and the turbulent flow parameter  $\sigma$  that depends on both wind  
 256 speed and local vegetation roughness.

257 In order to create the dispersal kernel, we first take the wind speeds at measure-  
 258 ment height  $z_m$  and correct them to find wind speed  $U$  for any height  $H$  by using the  
 259 logarithmic wind profile

$$260 \quad U = \frac{1}{H} \int_{d+z_0}^H \frac{u^*}{K} \log \left( \frac{z-d}{z_0} \right) dz \quad (3)$$

261 given in Bullock et al. (2012) equation 6, with the notation slightly modified. Here,  $z$   
 262 is the height above the ground,  $K$  is the von Karman constant, and  $u^*$  is the friction  
 263 velocity. The zero-plane displacement  $d$  and roughness length  $z_0$  are surface roughness  
 264 parameters that, for a grass canopy height  $h$  above the ground, are approximated by  
 265  $d \approx 0.7h$  and  $z_0 \approx 0.1h$ . These estimates are from Raupach (1994) for a canopy area  
 266 index  $\Lambda = 1$  in which the sum of grass canopy elements is equal to the unit area being  
 267 measured. A 0.15 m grass height at the study site gives  $d = 0.105$  and  $z_0$ , which are  
 268 suitable approximations for grassland (Wiernga, 1993). Calculations of  $u^*$  were done  
 269 using equation A2 from Skarpaas and Shea (2007), in which

$$270 \quad u^* = KU_m \left[ \log \left( \frac{z_m - d}{z_0} \right) \right]^{-1} \quad (4)$$

271 and  $U_m$  is the mean wind velocity at the measurement height  $z_m$ . Values for the turbulent  
 272 flow parameter  $\sigma$  were then calculated using the estimate made by Skarpaas and Shea

273 (2007) in their equation A4, where

$$274 \quad \sigma = 2A_w^2 \sqrt{\frac{K(z-d)u^*}{C_0 U}} \quad (5)$$

275 and  $C_0$  is the Kolmogorov constant.  $A_w$  is a constant that relates vertical turbulence  
 276 to friction velocity and is approximately equal to 1.3 under the assumptions of above-  
 277 canopy flow made by Skarpaas and Shea (2007), based off calculations from Hsieh and  
 278 Katul (1997). In addition, the assumption that  $z = H$  was made in order to make the  
 279 calculation of  $\sigma$  more feasible.

280 The values from the previous three equations give us the necessary information to  
 281 calculate  $\mu'$  and  $\lambda'$ , thus allowing us to create the WALD distribution  $p(r)$ . However, the  
 282 base WALD model does not take into account variation in wind speeds or seed terminal  
 283 velocities, which limits its applicability in systems where such variation is present. In  
 284 order to account for this variation, we integrate the WALD model over distributions these  
 285 two variables using the same method as Skarpaas and Shea (2007). The WALD model  
 286 assumes seed release from a single point source, though, which is not realistic for a shrub;  
 287 because seeds are released across the entire height of the shrub rather than from a point  
 288 source,  $p(r)$  was also integrated across the uniform distribution from the grass canopy  
 289 height to the shrub height. Thus, under the assumptions that the height at which a  
 290 seed is located does not affect its probability of being released and that seeds are evenly  
 291 distributed throughout the shrub, this gives the dispersal kernel  $K(r)$ , where

$$292 \quad K(r) = \iiint p(F)p(U)p(z)p(r) dF dU dz \quad (6)$$

293 and  $p(F)$  and  $p(U)$  are the PDFs of the terminal velocity  $F$  and wind speed  $U$ , respec-  
 294 tively, and  $p(z)$  is the uniform distribution from  $h$  to  $H$ .

295 The distribution  $p(F)$  in the integral above was constructed using experimentally  
 296 determined seed terminal velocities. This was done by using a high-speed camera and

297 motion tracking software to determine position as a function of time, and then using the  
 298 Levenberg-Marquardt algorithm to solve a quadratic-drag equation of motion for  $F$ . Be-  
 299 fore seeds were released, they were dried and then dyed with yellow fluorescent powder,  
 300 and then put against a black background to improve visibility and make tracking easier.  
 301 While the powder added mass to the seeds, this added mass only yielded an approxi-  
 302 mately 2.5% increase and was thus negligible, likely having little effect on their terminal  
 303 velocities. Measurements were conducted for 48 seeds that were randomly chosen from a  
 304 seed pool derived from different plants, and then an empirical PDF of terminal velocities  
 305 was constructed using the data. Constructing  $p(U)$  involved creating an empirical PDF  
 306 of hourly wind speeds at Five Points, the site closest to the 12 transects being used,  
 307 that were obtained from meteorological data collected at the Seville National Wildlife  
 308 Refuge from 1988 to 2010. We did not weight  $p(U)$  and assumed that the probability  
 309 seed release from the shrub is the same regardless of wind speed.

### 310 **Spatial integral projection model**

311 Given that the shrub population at this site is approximately homogeneous perpendic-  
 312 ular to the direction of encroachment, expansion is modelled as a wave moving in one  
 313 dimension. A spatial integral projection model (SIPM) is used to estimate the speed at  
 314 which encroachment occurs; such a model incorporates the effects of variation in traits  
 315 like plant size that stage-structured models, such as those described in Neubert and  
 316 Caswell (2000), do not capture. According to Jongejans et al. (2011), a general SIPM  
 317 can be formulated as

$$318 \quad \mathbf{n}(x_2, z_2, t + 1) = \iint \tilde{K}(x_2, x_1, z_2, z_1) \mathbf{n}(x_1, z_1, t) dx_1 dz_1 \quad (7)$$

319 where  $x_1$  and  $x_2$  are locations of individuals of a particular size before and after one unit of  
 320 time, and  $z_1$  and  $z_2$  are the respective sizes. The vector  $\mathbf{n}$  indicates the population density

of each size, and  $\tilde{K}$  is a kernel that combines dispersal with demography. Though this SIPM represents a continuous spectrum of shrub sizes and densities, it was implemented by discretising the above integral with a 200 x 200 matrix, as this makes calculations significantly more tractable.

Movement of the wave is determined by the components of the combined dispersal/demography kernel  $\tilde{K}$ , which is of the same form as that used in Jongejans et al. (2011). Here,

$$\tilde{K}(x_2, x_1, z_2, z_1) = K(x_2 - x_1)Q(z_2 - z_1) + \delta(x_2 - x_1)G(z_2 - z_1) \quad (8)$$

and  $K$  is the dispersal kernel,  $Q$  a reproduction function,  $G$  a growth function, and  $\delta$  the Dirac delta function.  $G$  is derived from the model for annual growth ratio, and  $Q$  is derived from the reproductive structures model as well as other factors including number of seeds per reproductive structure, probability of recruitment from seed, and recruit size. Both  $G$  and  $Q$  give the probability of transition between sizes; in the case of  $G$ , this is the probability of growing from one specific size to another, and in the case of  $Q$  the probability that an individual of a specific size produces a recruit of a specific size. The product of  $K$  and  $Q$  represents the production and dispersal of motile propagules, while the product of  $G$  and  $\delta$  represents the growth of sessile individuals.

Given growth function  $G$  and the reproduction function  $Q$ , the speed of the moving wave can be calculated as

$$c^* = \min_{s>0} \left[ \frac{1}{s} \ln(\rho_s) \right] \quad (9)$$

where  $s$  is the wave shape parameter and  $\rho_s$  is the dominant eigenvalue of the kernel  $\mathbf{H}_s$  (Jongejans et al., 2011). This estimate for the wavespeed is valid under the assumption that population growth decreases monotonically as conspecific density increases, with the highest rates of growth occurring at the lowest population densities (Lewis et al., 2006).



345 The kernel  $\mathbf{H}_s$  is defined as

$$346 \quad \mathbf{H}_s = M(s)Q(z_2 - z_1) + G(z_2 - z_1) \quad (10)$$

347 where  $M(s)$  is the moment-generating function of the dispersal kernel (Jongejans et al.,  
348 2011). For one-dimensional dispersal, this moment-generating function can be estimated  
349 as

$$350 \quad M(s) = \frac{1}{N} \sum_{i=1}^n I_0(sr_i) \quad (11)$$

351 where  $r$  is the dispersal distance for each observation, and  $I_0$  is the modified Bessel  
352 function of the first kind and zeroth order (Skarpaas and Shea, 2007). In order to obtain  
353  $M$ , numerous dispersal distances were simulated from the dispersal kernel  $K(r)$  described  
354 in the previous section, with over 2000 replications for each shrub height increment of 1  
355 cm. This was performed over the range from the lowest possible dispersal height to the  
356 maximum shrub height. Once  $M(s)$  was obtained for dispersal at each shrub height,  $\mathbf{H}_s$   
357 and  $c^*$  were calculated for each value of  $s$ ; this was done for values of  $s$  ranging from 0  
358 to 2, as it is this range in which  $c^*$  occurs.

359 Estimates of the wavespeed were bootstrapped for a total of 1000 replicates. Each  
360 bootstrap replicate recreated size- and density-dependent demographic models using 80%  
361 resampling on the original demographic data, and recreated dispersal kernels also using  
362 80% resampling on the wind speeds and seed terminal velocities. Between replicates,  
363 the structure of the demographic models was kept constant, though coefficient estimates  
364 were not; this approach, while effectively ignoring model uncertainty, has the benefit of  
365 increasing computational efficiency, which is especially useful given the time-consuming  
366 nature of numerically estimating the many dispersal kernels used in the model.

## 367 Results

### 368 Encroachment re-surveys

369 Figure 2.

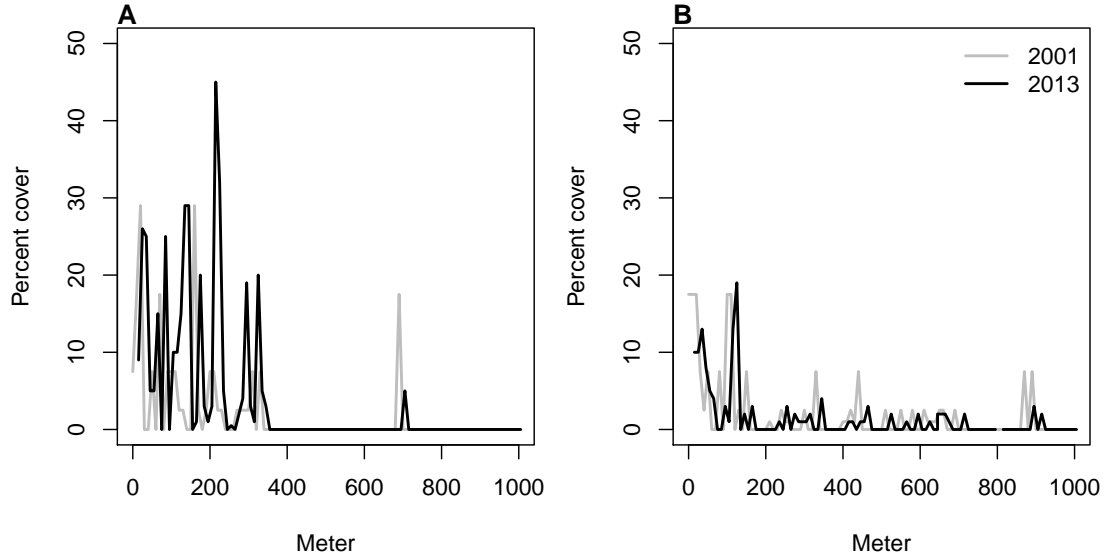


Figure 2: Re-surveys of shrub cover along two permanent trasects (A,B) surveyed in 2001 and 2013.

370 The speed of encroachment at the study site as estimated by the SIPM is rather  
 371 slow; as can be seen in Figure 3, the low-density wavefront moves at approximately  
 372 0.5 cm/yr under normal conditions and at 1 cm/yr under the best seedling survival  
 373 conditions observed in the dataset. These improved conditions were observed due to  
 374 above-average rainfall that occurred after greenhouse-grown seedlings were transplanted  
 375 to the site. Population growth in this low-density region of the moving wave is also low,  
 376 with a geometric growth rate of  $\lambda \approx 1.006$  and even lower rates of growth the higher-  
 377 density regions behind; in the higher-survival scenario the maximum rate increases to  
 378  $\lambda \approx 1.013$ , with growth still decreasing as density increases. For both scenarios, the  
 379 decrease in population growth rate with increasing density was monotonic across the  
 380 range of observed standardised densities, as is shown in Figure 3. This suggests that

381 an Allee effect is likely not present in this population, as the highest rate of population  
 382 growth is found at the lowest density vanguard of the encroaching population. Thus, the  
 383 conditions necessary for equation 9 to be valid are satisfied, and these wavespeeds are  
 384 applicable for a pulled-wave scenario in which no Allee effects are present.

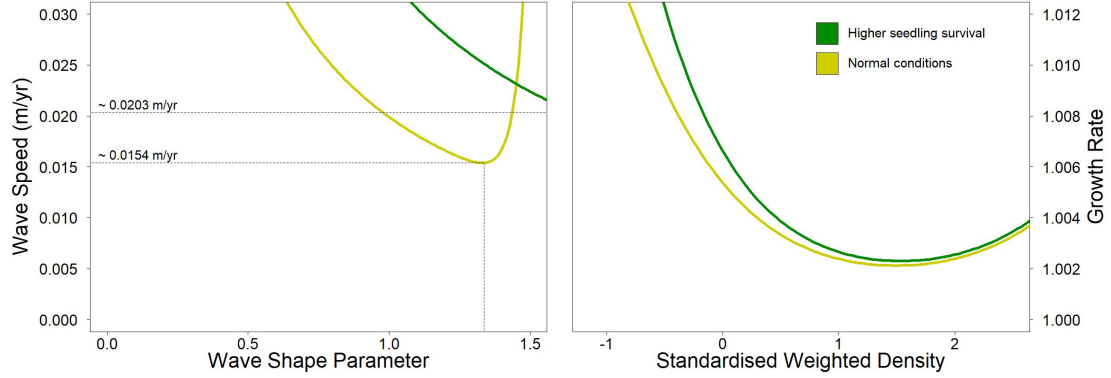


Figure 3: Estimated encroachment wave speeds (left) and geometric rates of population growth (right) for higher post-rainfall seedling survival and normal conditions.

385 As the speed of encroachment is quite limited, so is the extent of wind dispersal.  
 386 Long distance dispersal events, while more common for taller shrubs than their shorter  
 387 counterparts, are still uncommon overall. For the tallest shrub height of 1.98 m, only  
 388 0.32% of propagules exceed a dispersal distance of 5 m, and 0.02% exceed 10 m. At 1  
 389 m, or approximately half the tallest shrub height, long distance dispersal is even less  
 390 likely, with 0.0046% of propagules exceeding a dispersal distance of 5 m and 0.0009%  
 391 exceeding 10 m. Given that the median shrub height is only 0.64 m, the occurrence of  
 392 long-distance wind dispersal in most of the shrub population is highly improbable, and  
 393 the few instances in which it occurs will only be limited to the tallest shrubs. Thus, as  
 394 Figure 4 demonstrates, shorter dispersal distances dominate; even for the tallest shrub,  
 395 81% of seeds fall within only a metre of the plant, and this percentage increases as  
 396 shrub height decreases. Dispersal kernels have their highest probability density at dis-  
 397 persal distances between 2 and 8 cm from the shrub; here, as shrub height increases, the

398 most probable dispersal distance slightly increases while maximum probability density  
 399 decreases. Regardless of the shrub height, most dispersal will occur very close to the  
 400 plant, though increases in shrub height dramatically increase the likelihood of dispersal  
 401 at longer distances. It is clear that the shape of the height-dependent dispersal kernel  
 402  $K(r)$  varies greatly among the shrub population given the large range of shrub heights  
 403 observed; shrubs at lower heights have more slender kernels with most of the seeds dis-  
 404 persing closer to the plant, while taller shrubs have kernels with much fatter tails and  
 405 are more capable of longer-distance dispersal.

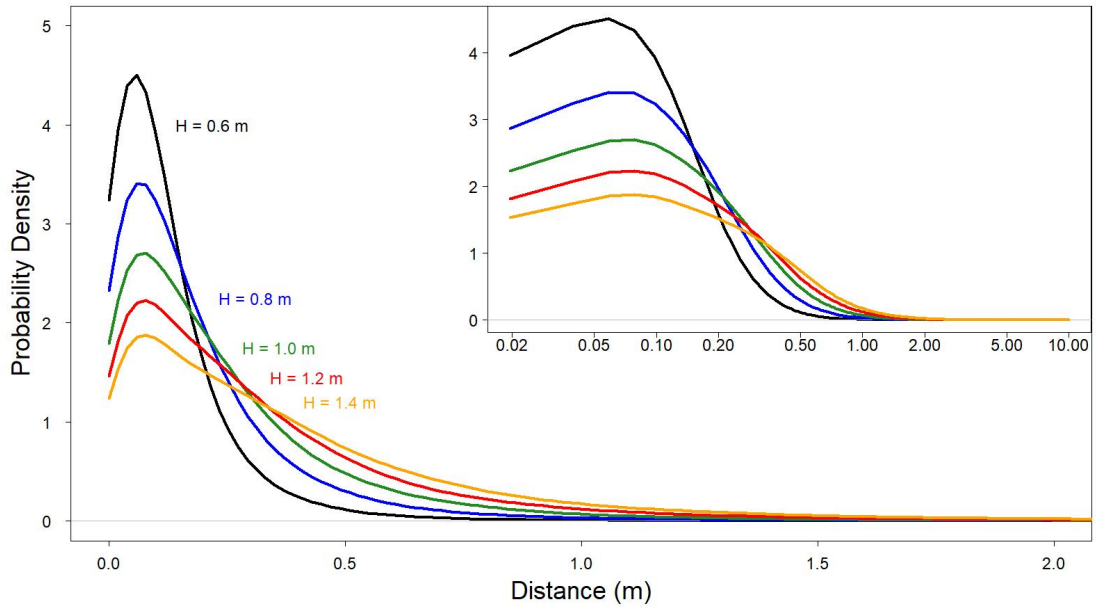


Figure 4: Dispersal kernels, with each colour representing a selected shrub height. The inset plot is the same as the large plot, though with a logarithmic x-axis to more easily show differences in dispersal probability at smaller distances.

406 Density and size dependence are evident in all 4 of the demographic rates, with  
 407 coefficients for each model displayed in Table 2. For growth, reproduction, and survival,  
 408 density dependence is mostly negative and monotonic; this is not the case for probability  
 409 of flowering, where shrub size seems to be more important than the effects of density alone

410 and suggests that larger shrubs have a higher probability of flowering than their smaller  
411 counterparts. This, along with size and density dependence in growth and reproduction,  
412 is shown in Figure 5. Size dependence is positive for reproduction, as would be expected  
413 since larger plants typically produce more flowers and fruits. However, annual growth  
414 decreases as size increases; this could be in part due to the annual growth in this study  
415 being quantified as a proportion relative to the shrub's initial size. While larger shrubs  
416 may produce more plant material over a year in terms of absolute volume, smaller shrubs  
417 produce less but can still have higher annual growth in terms of the percentage of volume  
418 added relative to their initial volume. When compared to density, shrub size is a much  
419 stronger predictor of survival, with significant differences in mortality rates depending on  
420 shrub size. For small shrubs, mortality is exceptionally high, and increases in volume for  
421 these shrubs only slightly increase the likelihood of survival. However, after shrubs reach  
422 a logarithmic volume of approximately 7.3, they are almost guaranteed to survive, with  
423 survival rates near 100% persisting regardless of any further size increases. Interestingly,  
424 though most recruits were found at lower densities, the probability of recruitment from  
425 seed displays positive density dependence; the probability of recruitment was still very  
426 low, though, with a baseline rate of approximately 2 recruits per 10,000 seeds.

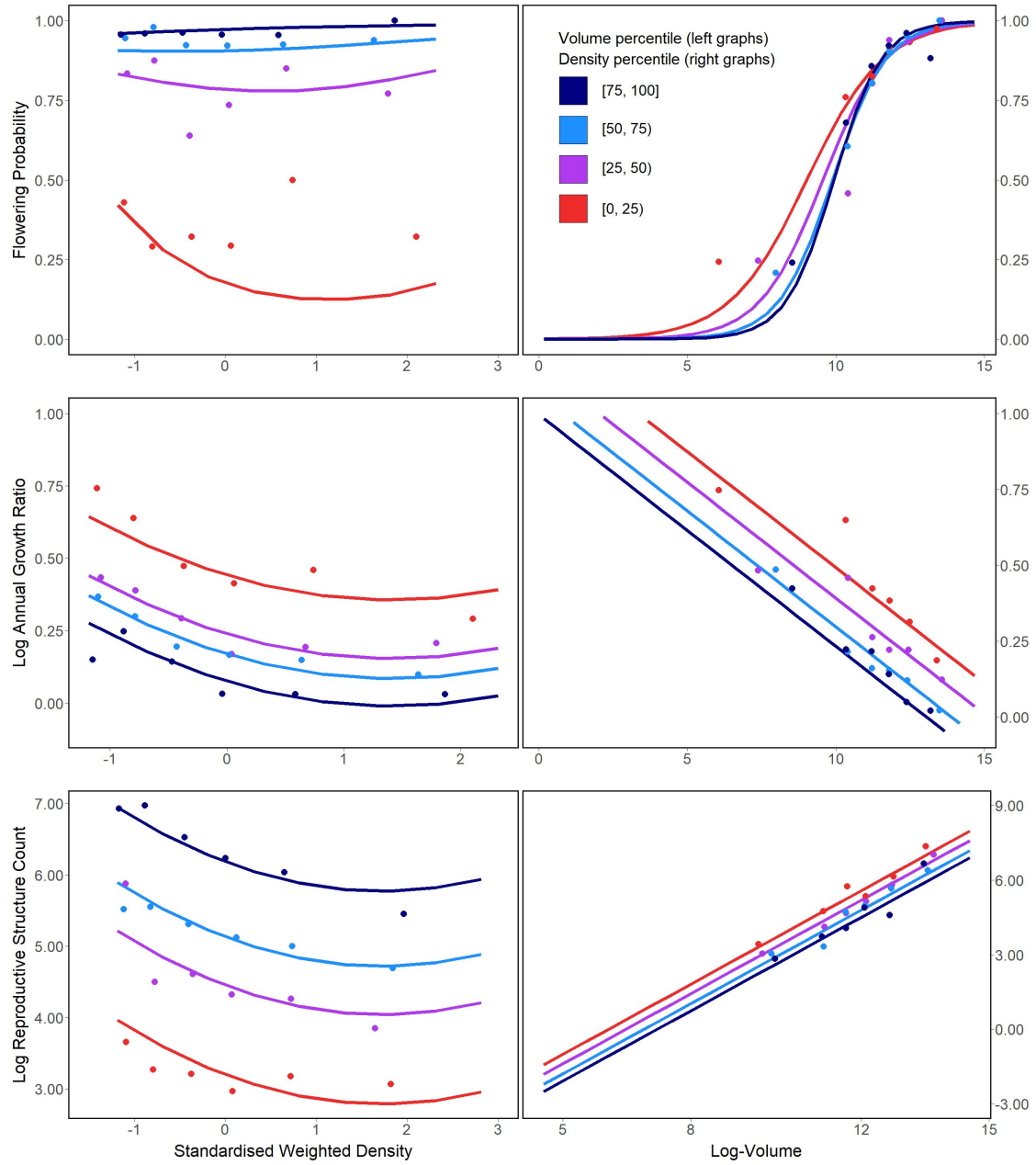


Figure 5: Flowering probability (top row), log annual growth ratio (centre row), and log reproductive structure count (bottom row) at all four sampling sites. In the left column of graphs, the three response variables are shown as a function of density for each of four volume quartiles, with each quartile containing six density bins; in the right column, the opposite occurs, with response variables shown as functions of four volume quartiles that each contain six density bins. Graphs quantifying the number of reproductive structures include data only on plants that flowered.

## Discussion

The slow movement of the encroaching creosotebush wave at the Sevilleta LTER site can likely be contributed to a combination of three factors: short dispersal distances with extremely limited long-distance dispersal events, very low probability of recruitment from seed, and high seedling mortality. These three barriers, when combined, form a formidable challenge to the establishment of new shrubs at the low-density front of the wave. First, a seed must travel far enough to avoid competition with the parent shrub, which is unlikely given the dispersal kernels shown in Figure 2. Even if the seed manages to be dispersed this far, its chances of becoming a seedling are low. Caching and consumption by seed-eaters such as a variety of seed-harvesting ants (Whitford, 1978; Whitford et al., 1980; Lei, 1999) and the kangaroo rat *Dipodomys merriami* (Chew and Chew, 1970) decreases the amount of seeds available for germination. However, reduction in germination caused by destruction of seeds may be partly mitigated by the more favourable germination conditions that these seeds can experience when cached underground (Chew and Chew, 1970). Many of the remaining seeds will still fail to germinate, and in the unlikely event that germination does occur, seedlings will likely die given the high rates of mortality observed in smaller shrubs. Such high rates of creosotebush seedling mortality have been observed in other studies as well (Boyd and Brum, 1983; Bowers et al., 2004), probably due to a combination of herbivory, competition, and abiotic stresses.

However, as low as they are, the wavespeed estimates given in this paper are still conservative estimates for reasons mostly related to dispersal. First, it is important to note that the dispersal kernels used here, while they account for variation in factors such as wind speed and terminal velocity, may underestimate the distances that shrub propagules travel. Because the WALD model assumes that terminal velocity is reached immediately upon seed release, seeds in the estimate thus take a shorter time to fall

453 and have less time to be transported by wind, and the true frequency of long-distance  
454 dispersal events may thus be greater than what is estimated here. Second, dispersal at the  
455 study site could occur through additional mechanisms other than wind. For example,  
456 secondary dispersal through runoff from significant rainfall events can transport seeds  
457 (Thompson et al., 2014), and given that long-distance dispersal by bird and subsequent  
458 species divergence is thought to be responsible for creosotebush being in North America  
459 in the first place (Wells and Hunziker, 1976), short-distance dispersal by other animals  
460 at the study site likely occurs. As mentioned above, seeds are transported by seed-  
461 harvesting ants and granivorous mammals, where they are often stored in caches that  
462 can be appreciable distances from the parent shrubs. Whether transportation occurs via  
463 ant or rodent, creosotebush seeds can be moved significantly further than wind alone  
464 can, though many of these seeds are eventually consumed.

465 Despite the more conservative estimates our model yields, the estimated rate of dis-  
466 persal in creosotebush populations at the Sevilleta National Wildlife Refuge is consistent  
467 with observations from the past 50-60 years, as creosotebush expansion during this time  
468 has been minimal (Moreno-de las Heras et al., 2016). However, it cannot explain the  
469 long-term increases in creosotebush cover at the study site, as total encroachment over  
470 the past 150 years is much greater than what would be expected given the encroachment  
471 rates derived by our models. Such a discrepancy is likely due to much of the expansion  
472 occurring in an episodic fashion, with short times during which rapid encroachment oc-  
473 curs due to favourable environmental conditions. This could be due in part to seedling  
474 recruitment, which is a factor that strongly limits creosotebush expansion, being rare  
475 and episodic. For example, Allen et al. (2008) estimate that a major recruitment event  
476 occurred at this site in the 1950s, which is supported by photographic evidence from  
477 Milne et al. (2003) of a drought-driven expansion during this time. Moreno-de las Heras  
478 et al. (2016) estimate that after this expansion, several smaller creosotebush recruitment  
479 events occurred in decadal episodes. However, such events can be highly localised and



480 may not necessarily occur at the low-density front of encroachment, which could explain  
481 how these recruitment events can still coexist with lack of encroachment in the recent  
482 past.

483 Overall, our observations and model highlight three aspects of creosotebush encroach-  
484 ment that should be the focus of future studies seeking to obtain better estimates of  
485 encroachment rates. First, negative density dependence in survival, growth, and repro-  
486 duction is demonstrated, along with size dependence. The clear dependence on size and  
487 conspecific density suggests that they both should be considered when estimating cre-  
488 osotebush expansion and quantifying the demographic variation that contributes to it.  
489 Second, wind dispersal in these shrubs is quite limited; though the dispersal kernels seen  
490 here are typical in the sense that they are characterised by high near-plant dispersal and  
491 exceptionally low long-distance dispersal, the scale across which such dispersal occurs  
492 is small, with most seeds landing within only 1 m of the shrub. Wind dispersal alone  
493 may be an underestimate of the true amount of dispersal occurring, and future work  
494 should seek to incorporate the effects of dispersal by runoff and animals so that a more  
495 representative model of total dispersal can be obtained. Finally, encroachment is slow or  
496 even stagnates, but only most of the time. Though our encroachment speed estimates  
497 are representative of creosotebush populations for most years, the significant expansion  
498 seen over larger time scales suggests that there is episodic expansion in other years; while  
499 our model is consistent with the recent stagnation in creosotebush encroachment at the  
500 Sevilleta LTER site, a model that also includes interannual variability in factors such  
501 as survival and recruitment would be able to better account for instances of episodic  
502 population expansion that are characteristic of this location.

## 503 Acknowledgements

## 504 Author contributions

## 505 Data accessibility

## 506 References

- 507 Allen, A., W. Pockman, C. Restrepo, and B. Milne. 2008. Allometry, growth and  
508 population regulation of the desert shrub *Larrea tridentata*. *Functional Ecology* pages  
509 197–204.
- 510 Bowers, J. E., R. M. Turner, and T. L. Burgess. 2004. Temporal and spatial patterns in  
511 emergence and early survival of perennial plants in the Sonoran Desert. *Plant Ecology*  
512 **172**:107–119.
- 513 Boyd, R. S., and G. D. Brum. 1983. Postdispersal reproductive biology of a Mojave Desert  
514 population of *Larrea tridentata* (Zygophyllaceae). *American Midland Naturalist* pages  
515 25–36.
- 516 Brandt, J. S., M. A. Haynes, T. Kuemmerle, D. M. Waller, and V. C. Radeloff. 2013.  
517 Regime shift on the roof of the world: Alpine meadows converting to shrublands in  
518 the southern Himalayas. *Biological Conservation* **158**:116–127.
- 519 Buffington, L. C., and C. H. Herbel. 1965. Vegetational changes on a semidesert grassland  
520 range from 1858 to 1963. *Ecological monographs* **35**:139–164.
- 521 Bullock, J. M., S. M. White, C. Prudhomme, C. Tansey, R. Perea, and D. A. Hooftman.  
522 2012. Modelling spread of British wind-dispersed plants under future wind speeds in  
523 a changing climate. *Journal of Ecology* **100**:104–115.

524 Cabral, A., J. De Miguel, A. Rescia, M. Schmitz, and F. Pineda. 2003. Shrub encroach-  
525 ment in Argentinean savannas. *Journal of Vegetation Science* **14**:145–152.

526 Chew, R. M., and A. E. Chew. 1970. Energy relationships of the mammals of a desert  
527 shrub (*Larrea tridentata*) community. *Ecological Monographs* pages 2–21.

528 D’Odorico, P., J. D. Fuentes, W. T. Pockman, S. L. Collins, Y. He, J. S. Medeiros,  
529 S. DeWekker, and M. E. Litvak. 2010. Positive feedback between microclimate and  
530 shrub encroachment in the northern Chihuahuan desert. *Ecosphere* **1**:1–11.

531 D’Odorico, P., G. S. Okin, and B. T. Bestelmeyer. 2012. A synthetic review of feedbacks  
532 and drivers of shrub encroachment in arid grasslands. *Ecohydrology* **5**:520–530.

533 Gandhi, S. R., E. A. Yurtsev, K. S. Korolev, and J. Gore. 2016. Range expansions  
534 transition from pulled to pushed waves as growth becomes more cooperative in an  
535 experimental microbial population. *Proceedings of the National Academy of Sciences*  
536 **113**:6922–6927.

537 Gardner, J. L. 1951. Vegetation of the creosotebush area of the Rio Grande Valley in  
538 New Mexico. *Ecological Monographs* **21**:379–403.

539 Gibbens, R., R. McNeely, K. Havstad, R. Beck, and B. Nolen. 2005. Vegetation changes  
540 in the Jornada Basin from 1858 to 1998. *Journal of Arid Environments* **61**:651–668.

541 Goslee, S., K. Havstad, D. Peters, A. Rango, and W. Schlesinger. 2003. High-resolution  
542 images reveal rate and pattern of shrub encroachment over six decades in New Mexico,  
543 USA. *Journal of Arid Environments* **54**:755–767.

544 Grover, H. D., and H. B. Musick. 1990. Shrubland encroachment in southern New Mexico,  
545 USA: an analysis of desertification processes in the American Southwest. *Climatic*  
546 *change* **17**:305–330.

547 Hara, T. 1993. Mode of competition and size-structure dynamics in plant communities.  
548 Plant Species Biology **8**:75–84.

549 Hsieh, C.-I., and G. G. Katul. 1997. Dissipation methods, Taylor’s hypothesis, and  
550 stability correction functions in the atmospheric surface layer. Journal of Geophysical  
551 Research: Atmospheres **102**:16391–16405.

552 Huang, H., L. D. Anderegg, T. E. Dawson, S. Mote, and P. D’Odorico. 2020. Crit-  
553 ical transition to woody plant dominance through microclimate feedbacks in North  
554 American coastal ecosystems. Ecology **101**:e03107.

555 Jongejans, E., K. Shea, O. Skarpaas, D. Kelly, and S. P. Ellner. 2011. Importance of  
556 individual and environmental variation for invasive species spread: a spatial integral  
557 projection model. Ecology **92**:86–97.

558 Katul, G., A. Porporato, R. Nathan, M. Siqueira, M. Soons, D. Poggi, H. Horn, and  
559 S. A. Levin. 2005. Mechanistic analytical models for long-distance seed dispersal by  
560 wind. The American Naturalist **166**:368–381.

561 Keitt, T. H., M. A. Lewis, and R. D. Holt. 2001. Allee effects, invasion pinning, and  
562 species’ borders. The American Naturalist **157**:203–216.

563 Kelleway, J. J., K. Cavanaugh, K. Rogers, I. C. Feller, E. Ens, C. Doughty, and N. Sain-  
564 tilan. 2017. Review of the ecosystem service implications of mangrove encroachment  
565 into salt marshes. Global Change Biology **23**:3967–3983.

566 Knapp, A. K., J. M. Briggs, S. L. Collins, S. R. Archer, M. S. BRET-HARTE, B. E.  
567 Ewers, D. P. Peters, D. R. Young, G. R. Shaver, E. Pendall, et al. 2008. Shrub  
568 encroachment in North American grasslands: shifts in growth form dominance rapidly  
569 alters control of ecosystem carbon inputs. Global Change Biology **14**:615–623.

- 570 Kot, M., M. A. Lewis, and P. van den Driessche. 1996. Dispersal data and the spread of  
571 invading organisms. *Ecology* **77**:2027–2042.
- 572 Lei, S. A. 1999. Ecological impacts of *Pogonomyrmex* on woody vegetation of a *Larrea*-  
573 *Ambrosia* shrubland. *The Great Basin Naturalist* pages 281–284.
- 574 Lewis, M., and P. Kareiva. 1993. Allee dynamics and the spread of invading organisms.  
575 *Theoretical Population Biology* **43**:141–158.
- 576 Lewis, M. A., M. G. Neubert, H. Caswell, J. S. Clark, and K. Shea, 2006. A guide  
577 to calculating discrete-time invasion rates from data. Pages 169–192 *in* *Conceptual*  
578 *ecology and invasion biology: reciprocal approaches to nature*. Springer.
- 579 Mabry, T. J., J. H. Hunziker, D. Difeo Jr, et al. 1978. Creosote bush: biology and  
580 chemistry of *Larrea* in New World deserts. Dowden, Hutchinson & Ross, Inc.
- 581 Maddox, J. C., and S. Carlquist. 1985. Wind dispersal in Californian desert plants:  
582 experimental studies and conceptual considerations. *Aliso: A Journal of Systematic*  
583 *and Evolutionary Botany* **11**:77–96.
- 584 Marshall, A. K., 1995. *Larrea tridentata*. URL [https://www.fs.fed.us/database/](https://www.fs.fed.us/database/feis/plants/shrub/lartri/all.html#8)  
585 [feis/plants/shrub/lartri/all.html#8](https://www.fs.fed.us/database/feis/plants/shrub/lartri/all.html#8).
- 586 Milne, B. T., D. I. Moore, J. L. Betancourt, J. A. Parks, T. W. Swetnam, R. R. Par-  
587 menter, and W. T. Pockman. 2003. Multidecadal drought cycles in south-central New  
588 Mexico: Patterns and consequences. Oxford University Press: New York, NY.
- 589 Moreno-de Las Heras, M., R. Díaz-Sierra, L. Turnbull, and J. Wainwright. 2015. Assess-  
590 ing vegetation structure and ANPP dynamics in a grassland–shrubland Chihuahuan  
591 ecotone using NDVI–rainfall relationships. *Biogeosciences* **12**:2907–2925.
- 592 Moreno-de las Heras, M., L. Turnbull, and J. Wainwright. 2016. Seed-bank structure

593 and plant-recruitment conditions regulate the dynamics of a grassland-shrubland Chi-  
594 huahuan ecotone. *Ecology* **97**:2303–2318.

595 Mugasi, S., E. Sabiiti, and B. Tayebwa. 2000. The economic implications of bush  
596 encroachment on livestock farming in rangelands of Uganda. *African Journal of Range  
597 and Forage Science* **17**:64–69.

598 Nathan, R., G. G. Katul, G. Bohrer, A. Kuparinen, M. B. Soons, S. E. Thompson,  
599 A. Trakhtenbrot, and H. S. Horn. 2011. Mechanistic models of seed dispersal by wind.  
600 *Theoretical Ecology* **4**:113–132.

601 Neubert, M. G., and H. Caswell. 2000. Demography and dispersal: calculation and  
602 sensitivity analysis of invasion speed for structured populations. *Ecology* **81**:1613–  
603 1628.

604 Oba, G., E. Post, P. Syvertsen, and N. Stenseth. 2000. Bush cover and range condition  
605 assessments in relation to landscape and grazing in southern Ethiopia. *Landscape  
606 ecology* **15**:535–546.

607 Pan, S., and G. Lin. 2012. Invasion traveling wave solutions of a competitive system  
608 with dispersal. *Boundary Value Problems* **2012**:120.

609 Parizek, B., C. M. Rostagno, and R. Sottini. 2002. Soil erosion as affected by shrub  
610 encroachment in northeastern Patagonia. *Rangeland Ecology & Management/Journal  
611 of Range Management Archives* **55**:43–48.

612 Peters, D. P., and J. Yao. 2012. Long-term experimental loss of foundation species:  
613 consequences for dynamics at ecotones across heterogeneous landscapes. *Ecosphere*  
614 **3**:1–23.

615 Ratajczak, Z., J. B. Nippert, and S. L. Collins. 2012. Woody encroachment decreases  
616 diversity across North American grasslands and savannas. *Ecology* **93**:697–703.

- 617 Raupach, M. 1994. Simplified expressions for vegetation roughness length and zero-  
618 plane displacement as functions of canopy height and area index. *Boundary-Layer*  
619 *Meteorology* **71**:211–216.
- 620 Ravi, S., P. D’Odorico, S. L. Collins, and T. E. Huxman. 2009. Can biological invasions  
621 induce desertification? *The New Phytologist* **181**:512–515.
- 622 Reed, M., L. Stringer, A. Dougill, J. Perkins, J. Atlhopheng, K. Mulale, and N. Favretto.  
623 2015. Reorienting land degradation towards sustainable land management: Linking  
624 sustainable livelihoods with ecosystem services in rangeland systems. *Journal of envi-*  
625 *ronmental management* **151**:472–485.
- 626 Reynolds, J. F., R. A. Virginia, P. R. Kemp, A. G. De Soyza, and D. C. Tremmel. 1999.  
627 Impact of drought on desert shrubs: effects of seasonality and degree of resource island  
628 development. *Ecological Monographs* **69**:69–106.
- 629 Roques, K., T. O’connor, and A. R. Watkinson. 2001. Dynamics of shrub encroach-  
630 ment in an African savanna: relative influences of fire, herbivory, rainfall and density  
631 dependence. *Journal of Applied Ecology* **38**:268–280.
- 632 Schlesinger, W. H., and A. M. Pilmanis. 1998. Plant-soil interactions in deserts. *Biogeo-*  
633 *chemistry* **42**:169–187.
- 634 Schlesinger, W. H., J. A. Raikes, A. E. Hartley, and A. F. Cross. 1996. On the spatial  
635 pattern of soil nutrients in desert ecosystems: ecological archives E077-002. *Ecology*  
636 **77**:364–374.
- 637 Schlesinger, W. H., J. F. Reynolds, G. L. Cunningham, L. F. Huenneke, W. M. Jarrell,  
638 R. A. Virginia, and W. G. Whitford. 1990. Biological feedbacks in global desertification.  
639 *Science* **247**:1043–1048.

- 640 Sirami, C., and A. Monadjem. 2012. Changes in bird communities in Swaziland savannas  
641 between 1998 and 2008 owing to shrub encroachment. *Diversity and Distributions*  
642 **18**:390–400.
- 643 Skarpaas, O., and K. Shea. 2007. Dispersal patterns, dispersal mechanisms, and invasion  
644 wave speeds for invasive thistles. *The American Naturalist* **170**:421–430.
- 645 Sullivan, L. L., B. Li, T. E. Miller, M. G. Neubert, and A. K. Shaw. 2017. Density depen-  
646 dence in demography and dispersal generates fluctuating invasion speeds. *Proceedings*  
647 *of the National Academy of Sciences* **114**:5053–5058.
- 648 Taylor, C. M., and A. Hastings. 2005. Allee effects in biological invasions. *Ecology*  
649 *Letters* **8**:895–908.
- 650 Thompson, S. E., S. Assouline, L. Chen, A. Trahtenbrot, T. Svoray, and G. G. Katul.  
651 2014. Secondary dispersal driven by overland flow in drylands: Review and mechanistic  
652 model development. *Movement ecology* **2**:7.
- 653 Trollope, W., F. Hobson, J. Danckwerts, and J. Van Niekerk. 1989. Encroachment and  
654 control of undesirable plants. *Veld management in the Eastern Cape* pages 73–89.
- 655 Turnbull, L., J. Wainwright, and R. E. Brazier. 2010. Changes in hydrology and erosion  
656 over a transition from grassland to shrubland. *Hydrological Processes: An Interna-*  
657 *tional Journal* **24**:393–414.
- 658 Van Auken, O. 2009. Causes and consequences of woody plant encroachment into western  
659 North American grasslands. *Journal of environmental management* **90**:2931–2942.
- 660 Van Auken, O. W. 2000. Shrub invasions of North American semiarid grasslands. *Annual*  
661 *review of ecology and systematics* **31**:197–215.
- 662 Vasek, F. C. 1980. Creosote bush: Long-lived clones in the Mojave Desert. *American*  
663 *Journal of Botany* **67**:246–255.



- 664 Veit, R. R., and M. A. Lewis. 1996. Dispersal, population growth, and the Allee ef-  
665 fect: dynamics of the house finch invasion of eastern North America. *The American*  
666 *Naturalist* **148**:255–274.
- 667 Wang, M.-H., M. Kot, and M. G. Neubert. 2002. Integrodifference equations, Allee  
668 effects, and invasions. *Journal of mathematical biology* **44**:150–168.
- 669 Weiner, J. 1990. Asymmetric competition in plant populations. *Trends in ecology &*  
670 *evolution* **5**:360–364.
- 671 Wells, P. V., and J. H. Hunziker. 1976. Origin of the creosote bush (*Larrea*) deserts of  
672 southwestern North America. *Annals of the Missouri Botanical Garden* pages 843–861.
- 673 Whitford, W., E. Depree, and P. Johnson. 1980. Foraging ecology of two chihuahuan  
674 desert ant species: *Novomessor cockerelli* and *Novomessor albisetosus*. *Insectes Sociaux*  
675 **27**:148–156.
- 676 Whitford, W. G. 1978. Structure and seasonal activity of Chihuahua desert ant commu-  
677 nities. *Insectes Sociaux* **25**:79–88.
- 678 Wiernga, J. 1993. Representative roughness parameters for homogeneous terrain.  
679 *Boundary-Layer Meteorology* **63**:323–363.